Re-Ingestion of Upstream Egress in a 1.5-Stage Gas Turbine Rig

James A Scobie, Fabian P Hualca, Marios Patinios, Carl M Sangan, J Michael Owen and Gary D Lock
j.a.scobie@bath.ac.uk, f.hualca@bath.ac.uk, m.patinios@bath.ac.uk,
c.m.sangan@bath.ac.uk, j.m.owen@bath.ac.uk and g.d.lock@bath.ac.uk
Department of Mechanical Engineering
University of Bath
Bath, BA2 7AY
United Kingdom

ABSTRACT

In gas turbines, rim seals are fitted at the periphery of stator and rotor discs to minimise the purge flow required to seal the wheel-space between the discs. *Ingestion* (or ingress) of hot mainstream gases through rim seals is a threat to the operating life and integrity of highly-stressed components, particularly in the first-stage turbine. Egress of sealing flow from the first-stage can be *re-ingested* in downstream stages.

This paper presents experimental results using a 1.5-stage test facility designed to investigate ingress into the wheel-spaces upstream and downstream of a rotor disc. Re-ingestion was quantified using measurements of CO_2 concentration, with seeding injected into the upstream and downstream sealing flows. Here a theoretical mixing model has been developed from first principles and validated by the experimental measurements. For the first time, a method to quantify the mass fraction of the fluid carried over from upstream egress into downstream ingress has been presented and measured; it was shown that this fraction increased as the downstream sealing flow rate increased. The upstream purge was shown to not significantly disturb the fluid dynamics but only partially mixes with the annulus flow near the downstream seal, with the ingested fluid emanating from the boundary layer on the blade platform. From the analogy between heat and mass transfer, the measured mass-concentration flux is

equivalent to an enthalpy flux and this re-ingestion could significantly reduce the adverse effect of ingress in the downstream wheel-space. Radial traverses using a concentration probe in and around the rim seal clearances provide insight into the complex interaction between the egress, ingress and mainstream flows.

1 INTRODUCTION

The gas turbine is a combustion engine that can convert natural gas or other liquid fuels to mechanical energy. This energy can be used to drive a generator that produces electrical energy, or form the core of an aero-engine. Designers have increased engine efficiency by raising the turbine entry temperature (TET, sometimes referred to as turbine inlet temperature). The metal temperature of the highly-stressed rotating discs in the turbine is controlled using relatively cool sealing (or purge) flow diverted from the compressor. Insufficient cooling reduces the operating life and integrity of vulnerable components, but superfluous use diminishes the benefits of an increased TET. For context, halving the purge flow translates to a reduction of 500 kg of fuel per flight-hour for a Boeing 747 at altitude. [1].

The cool sealing air pressurises the disc cavities and reduces the ingestion (or ingress) of high-temperature gases entrained from the mainstream annulus through clearances between rotating and static parts. Rim seals are fitted at the periphery of the wheel-space formed between discs to minimise purge. Over the operating range of the engine the clearances in these rim seals is influenced by thermal expansion and centrifugal and pressure loads. Figure 1 illustrates a typical high-pressure axial turbine and the detail of a typical rim seal. The configuration and clearance of these seals are designed to be appropriate for the varying stages in the turbine, as well as the degree of the thermal expansion over the operational range of the engine.

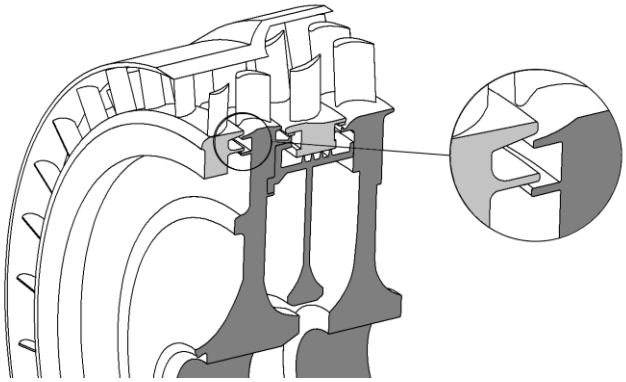

Figure 1: Typical rim seal in a high-pressure turbine

Re-ingestion occurs when a proportion of the egress of sealing flow from the first-stage wheel-space is entrained into the ingress into a downstream wheel-space. As the upstream egress is much cooler than the mainstream gas, re-ingestion could significantly reduce the adverse effect of ingress in the downstream stages. Ingress of hot gases can damage vulnerable components in the turbine.

There are two reasons why egress from the upstream wheel-space could affect ingress downstream. *Carry-over* is where the egress is not fully mixed with the mainstream so that the temperature of the fluid ingested (hence the enthalpy flux) into the downstream wheel-space is less than the fully-mixed value. *Disturbance* is a fluid-dynamic effect where the upstream egress disrupts the boundary layer near the downstream seal. This disturbance could occur even if the upstream egress were fully mixed with the mainstream flow, and the effect on downstream ingress could be adverse or favourable.

This paper presents experimental results using a 1.5-stage turbine rig designed to investigate ingress into the wheel-spaces upstream and downstream of a rotor disc. Engine-representative rim seals were tested under incompressible flow conditions ($Re_\phi \sim 10^6$, annulus Mach number ~ 0.4) over a range of purge-flow rates. Re-ingestion was

quantified using measurements of CO_2 concentration, with seeding injected into the upstream and downstream sealing flows. Section 2 describes the expected wheel-space flow structure with re-ingestion. Section 3 is a review of the relevant literature. Section 4 describes the theoretical equations used to interpret the concentration measurements and quantify the effects of re-ingestion. Section 5 describes the experimental facility and methods. Section 6 presents the results and the principal conclusions are given in Section 7.

2 ROTOR-STATOR SYSTEM AND RE-INGESTION

Figure 2 shows re-ingestion in a typical turbine stage with wheel-spaces upstream and downstream of the rotor. Consider first the flow structure in the upstream wheel-space, where there is a radial flow of sealing air with swirl, together with ingress and egress through the rim seal. The gap ratio, G, is sufficiently large to ensure separate boundary layers on the two discs. Fluid moves radially outward in the boundary layer on the rotor and inward in the boundary layer on the stator. Fluid moves axially across the rotating inviscid core from the stator to rotor with all radial flow confined to the boundary layers on the discs. In an outer region, there is an exchange of angular momentum and concentration (if the sealing flow is seeded with CO_2 in an isothermal experiment) between the ingress and egress. The outer region is the source for the flow in the boundary layer on the stator, and if the flow is fully mixed the concentration in the core should be equal to that on the stator walls with both distributions invariant with radius. This has been verified experimentally by Patinios *et al*. [2].

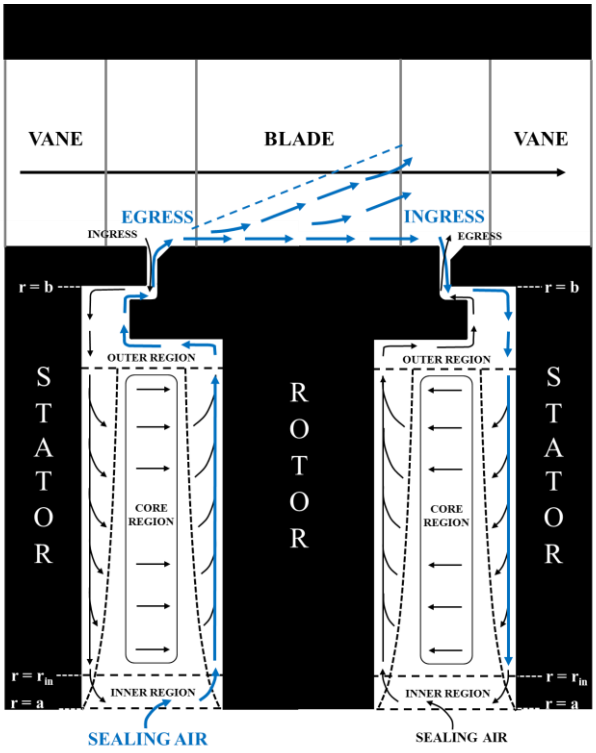

Figure 2: Flow structure demonstrating re-ingestion

Egress from the rim seal will propagate downstream through the blade passage. A proportion will be entrained into the passage vortex [3] and migrate radially in the annulus, and a proportion will be entrained as ingress into the downstream wheel-space.

The flow structure for the downstream wheel-space is a mirror-image of that upstream. However, the downstream egress pumped up the rotor side creates an axisymmetric jet that the ingress and re-ingestion from the mainstream must cross before the mixture of fluid is ingested into the wheel-space. There will be an exchange of angular momentum and chemical species (that is, CO_2) through the axisymmetric jet at the entrance to the seal; if the sealing flow is seeded, this will increase in the level of CO_2 concentration of the ingested fluid.

3 LITERATURE REVIEW

Scobie et al. [4] provide an extensive review of ingress in turbomachinery. Ingress is an inertial phenomenon governed by differences in pressure. Owen [5] developed a theoretical model to predict externally-induced ingress for inviscid, swirling flows and defined the sealing flow parameter, Φ_0:

$$\Phi_0 = \frac{C_{w,0}}{2\pi G_c \, \mathrm{Re}_\phi} = \frac{U}{\Omega b} \tag{3.1}$$

Here U is the bulk mean radial velocity of sealing air through the seal clearance and all other symbols are defined in the nomenclature. Sangan et al. [6] used the theoretical model to form an explicit relationship between Φ_0 and the effectiveness, ε:

$$\Theta_0 \equiv \frac{\Phi_0}{\Phi_{min}} = \frac{\varepsilon}{\left[1 + \Gamma_c^{-2/3}\left(1-\varepsilon\right)^{2/3}\right]^{3/2}} \tag{3.2}$$

Here Φ_{min} is the minimum flow rate to prevent ingress and Γ_c is the ratio of the discharge coefficients for ingress and egress. The equivalent equations for the non-dimensional ingress, Φ_i, and egress, Φ_e, are given by:

$$\Theta_i \equiv \frac{\Phi_i}{\Phi_{min}} = \frac{1-\varepsilon}{\left[1 + \Gamma_c^{-2/3}\left(1-\varepsilon\right)^{2/3}\right]^{3/2}} \tag{3.3}$$

and

$$\Theta_e \equiv \frac{\Phi_e}{\Phi_{min}} = \frac{1}{\left[1 + \Gamma_c^{-2/3}\left(1-\varepsilon\right)^{2/3}\right]^{3/2}} \tag{3.4}$$

Scobie *et al.* [4] did not review re-ingestion but to the authors' knowledge there are relatively few publications on this phenomenon. The possibility for recirculation of fluid ejected from upstream stator wells was postulated by Wisler [7] and Bayley and Childs [8], and studied computationally by Ozturk *et al.* [9]. Below is a short review of three publications related to the MAGPI programme [10].

Georgakis *et al.* [11] computationally investigated re-ingestion into a turbine stator-well, based on the experimental rig at Sussex. They showed that re-ingestion provided

a significant contribution to stator well cooling, calculating an increase in thermal effectiveness of 1 to 1.5% on the cavity walls due to the presence of the upstream egress.

Eastwood *et al.* [12] used the Sussex rig to experimentally investigate re-ingestion, attempting to assess if any cooling benefit could be gained in downstream stator wells from the cooling air ejected from upstream rim seals. Gas concentration measurements revealed that approximately 7% of the egress from the upstream wheel-space was re-ingested downstream under conditions with engine-representative sealing flow rates. The amount of re-ingestion reduced with increasing sealing flow.

Guijarro-Valencia *et al.* [13] presented the results of six separate CFD solutions which attempted to model the experiments conducted by Eastwood et al. They showed steady models failed to replicate any significant levels of re-ingestion, although a partial prediction was achieved using unsteady calculations. It was concluded that the fluid dynamics involved in the mixing of the sealing flow and the main gas path might were not accurately captured by steady computations, especially in regions near the rim seal where the mixing mechanisms were dominant.

4 THEORETICAL MODEL

In Section 6 re-ingestion has been quantified using measurements of CO_2 concentration, with seeding injected into the upstream and downstream sealing flows. This section describes a theoretical model used to interpret these experiments and to quantify the mass fraction of the re-ingested fluid.

4.1 Disturbance and carry-over

The sealing effectiveness, ε, can be defined in terms of the mass flow of ingress, egress and superposed sealing flow, $\dot{m}_i$, $\dot{m}_e$, and $\dot{m}0$:

$$\varepsilon = 1 - \frac{\dot{m}_i}{\dot{m}_e} = \frac{\dot{m}_0}{\dot{m}_e} \tag{4.1}$$

Here, concentration measurements (c) are used as a proxy and the concentration effectiveness is defined as

$$\varepsilon_c = \left(\frac{c_s - c_a}{c_0 - c_a} \right) \tag{4.2}$$

where the subscripts *a*, *0* and *s* respectively denote the values measured in the annulus, in the sealing flow at inlet to the wheel-space and on the stator - see Figure 3. As discussed in the introduction, disturbance is a fluid-dynamic effect where the upstream egress disrupts the pressure field near the downstream seal. It should be noted that this disturbance effect could alter both ε_d and consequently $\varepsilon_{c,d}$, whereas the addition of seeding to the upstream wheel-space should not alter ε_d. Here the subscripts *u* and *d* are used to denote the upstream and downstream wheel-spaces (Figure 3). It is assumed here that $\varepsilon_{c,u} = \varepsilon_u$, but, as discussed below, $\varepsilon_{c,d}$ is only equal to ε_d if it is defined correctly.

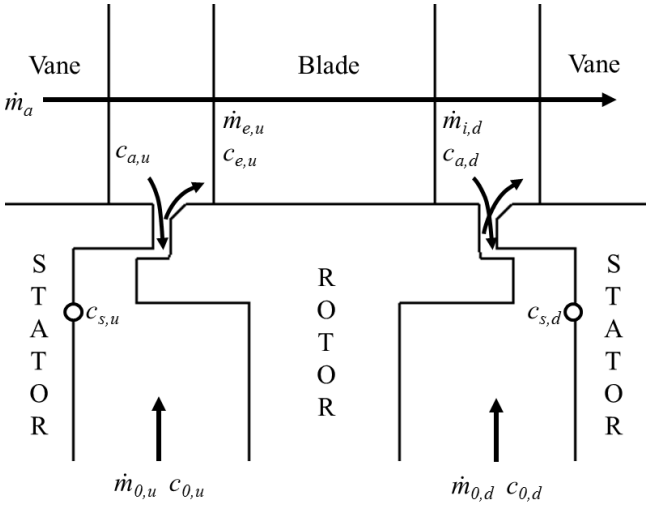

Figure 3: Simplified representation of mass flow rates and concentrations

Carry-over is where the seeded egress fluid is not fully mixed with the mainstream so that the concentration of the fluid ingested into the downstream wheel-space is greater than the fully-mixed value. To separate the disturbance and carry-over effects,

it is necessary to conduct two sets of experiments for a range of upstream and downstream sealing flow rates: one set without and one with seeding added to the upstream sealing flow. These are referred to below as the *upstream-unseeded* and *upstream-seeded* tests.

For the *upstream-unseeded* tests, if the measured effectiveness in the downstream wheel-space, $\varepsilon_{c,d}$, is invariant with $(\Phi_0/\Phi_{min})_u$ - and hence with ε_u - then the disturbance effect is not significant. However, if the upstream-unseeded tests do make a difference, so that ε_d depends on ε_u, the distribution of ε_d with $(\Phi_0/\Phi_{min})_d$ would need to be measured for different values of ε_u. The upstream-unseeded distributions of downstream effectiveness are referred to here as the datum cases, denoted by $\varepsilon^*_{c,d}$, with which the upstream-seeded distributions, $\varepsilon_{c,d}$, should be compared. That is,

$$\varepsilon^*_{c,d} = \left(\frac{c_s - c^*_a}{c_0 - c^*_a} \right)_d \tag{4.3}$$

where the downstream concentration in the annulus equals the upstream value, so that $c^*_{a,d} = c_{a,u}$.

For the *upstream-seeded* tests, if $\varepsilon_{c,d} > \varepsilon^*_{c,d}$ this implies that there has been a carry-over of upstream egress, which has increased the concentration of the fluid ingested from the annulus into the downstream wheel-space, so that $c_{a,d} > c^*_{a,d}$. If the downstream effectiveness is incorrectly based on the upstream concentration in the annulus, the measured value of $\varepsilon_{c,d}$ will not equal the true value of ε_d. To reconcile $\varepsilon_{c,d}$ and ε_d, it is necessary to define $\varepsilon_{c,d}$ on the *actual* concentration of the fluid ingested into the wheel-space, $c_{a,d}$. That is, $\varepsilon_{c,d}$ should be defined as

$$\varepsilon_{c,d} = \left(\frac{c_s - c_a}{c_0 - c_a} \right)_d \tag{4.4}$$

It follows that

$$c_{a,d} = \left(\frac{c_s - c_0 \varepsilon_c}{1 - \varepsilon_c} \right)_d \tag{4.5}$$

If $\varepsilon_{c,d} = \varepsilon_d = \varepsilon^*_{c,d}$, it follows that

$$c_{a,d} = \left(\frac{c_s - c_0 \varepsilon^*_c}{1 - \varepsilon^*_c} \right)_d \tag{4.6}$$

4.2 Concentration in the annulus

For *fully-mixed* flow in the annulus downstream of the rotor,

$$(\dot{m}_0 c_0)_u + (\dot{m}_a c_a)_u = (\dot{m}_0 + \dot{m}_a)_u \tilde{c}_{a,d} \tag{4.7}$$

That is, when seeding is added to the upstream sealing flow, the *mixed-out* concentration in the downstream annulus is given by

$$\tilde{c}_{a,d} = \frac{(\dot{m}_0 c_0)_u + (\dot{m}_a c_a)_u}{(\dot{m}_0 + \dot{m}_a)_u} \tag{4.8}$$

If there were no mixing in the annulus then the ingress from the boundary layer on the rotor platform would be entirely egress from upstream. Under these circumstances the fluid ingested into the downstream wheel-space would have the same concentration as that of the egress from the upstream wheel-space, $c_{e,u}$, where

$$c_{e,u} = \left(\varepsilon_c c_0 + (1 - \varepsilon_c) c_a \right)_u \tag{4.9}$$

4.3 Mass fraction of re-ingested fluid

Consider the control volume (CV) shown in Figure 4, located outside the downstream seal where the carry-over fluid from the upstream egress ($\dot{m}'$) mixes with the downstream egress ($\dot{m}_{e,d}$) and ingress ($\dot{m}_{i,d}$). After mixing, all the fluid is assumed to leave the CV with the same concentration, $c_{i,d} = c_{s,d}$; this would be the value measured on the downstream stator and representative of the core concentration in the wheel-space as presented in Figure 2.

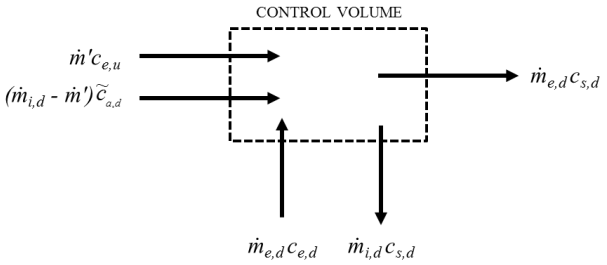

Figure 4: Representation of control volume

The total mass flow rate and the total mass-concentration entering and exiting the CV must be equal. The mass-concentration into the CV is:

$$(\dot{m}c)_{in} = \dot{m}' c_{e,u} + (\dot{m}_i - \dot{m}')\tilde{c}_{a,d} + (\dot{m}_e c_e)_d \tag{4.10}$$

The mass-concentration out of the CV is:

$$(\dot{m}c)_{out} = (\dot{m}_e c_s)_d + (\dot{m}_i c_s)_d \tag{4.11}$$

As

$$\dot{m}_{e,d} = (\dot{m}_0 + \dot{m}_i)_d \tag{4.12}$$

and

$$(\dot{m}c)_{e,d} = (\dot{m}_i c_s)_d + (\dot{m}_0 c_0)_d \tag{4.13}$$

it follows that

$$\dot{m}' c_{e,u} + (\dot{m}_{i,d} - \dot{m}')\tilde{c}_{a,d} + (\dot{m}_0 c_0)_d = \left((\dot{m}_0 + \dot{m}_i)c_s\right)_d \tag{4.14}$$

Hence, if $\dot{m}_{i,d} > 0$, the mass fraction is given by

$$\chi \equiv \frac{\dot{m}'}{\dot{m}_{i,d}} = \frac{c_{o,d} - c_{s,d}}{c_{e,u} - \tilde{c}_{a,d}} \left(\frac{c_{s,d} - \tilde{c}_{a,d}}{c_{0,d} - c_{s,d}} - \left(\frac{\dot{m}_0}{\dot{m}_i} \right)_d \right) \tag{4.15}$$

where

$$\left(\frac{\dot{m}_0}{\dot{m}_i} \right)_d = \left(\frac{\varepsilon^*}{1 - \varepsilon^*} \right)_d \tag{4.16}$$

In the limit when $\dot{m}_{0,d} = 0$, Eq (4.15) reduces to

$$\chi = \frac{c_{s,d} - \widetilde{c}_{a,d}}{c_{e,u} - \widetilde{c}_{a,d}} \tag{4.17}$$

4.4 Interpretation using analogy between heat and mass transfer

χ is the mass fraction of the upstream egress entrained into the downstream wheel-space. Using the analogy between heat and mass transfer, the mass-concentration flux, $\dot{m}'c_{e,u}$, is analogous to the enthalpy flux, $\dot{m}'h_{e,u}$, so that the concentration balance between the fluid carried over and the ingress into the downstream wheel-space is analogous to the enthalpy balance. In Section 6, χ is measured as a function of downstream sealing flow rate. (Strictly, the analogy is only valid for adiabatic flow, where the impermeable boundary condition for the concentration is equivalent to that for the temperature. In a turbine, the heat transfer to the carry-over fluid in the blade passage will attenuate the favourable effect of any re-ingestion.)

5 EXPERIMENTAL FACILITY

This section describes the measurement capability and operating conditions of the University of Bath research facility which experimentally models ingress into the upstream and downstream wheel-spaces of a 1.5-stage axial turbine. The rig was specifically designed for instrumentation access in a fluid-dynamically-scaled environment at low rotational Reynolds number and incompressible flow; the rig offers an efficient, flexible and relatively inexpensive means of assessing new rim seal design concepts. A comprehensive description of the rig design is provided by Patinios *et al.* [2].

The test section is shown in Figure 5. The turbine consists of 32 upstream vanes, 48 turned rotor blades, followed by a further 32 downstream vanes. The blade and vane geometries were designed by Siemens specifically for one of their engines. The

diameter of the disc to the underside of the rim seal shroud was 380 mm and the height of the annulus was 25 mm. The rotor disc and vanes were manufactured as a blisc and bladed-ring (respectively) and each machined from a single piece of titanium. The blisc could be rotated up to speeds of 4000 rpm by means of an asynchronous dynamometer, providing a rotational Reynolds number, $Re_\phi = 1.1 \times 10^6$. Detachable aluminium cover-plates on both the stationary and rotating sides of each wheel-space allowed for flexible operation and access.

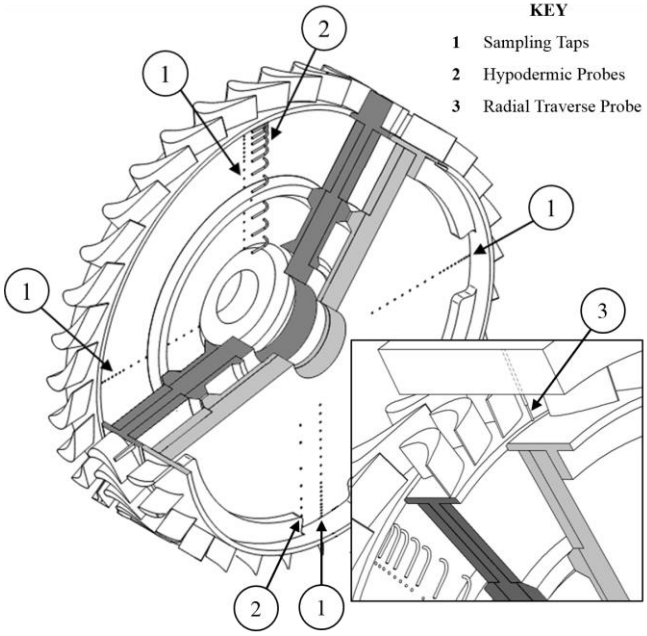

Figure 5: Test section and instrumentation

5.1 Operating conditions

Table 1 shows the two operating conditions used in the experiments. The flow exiting the vanes was virtually incompressible and near atmospheric pressure; the density, ρ, speed of sound, a, and air viscosity, μ, are determined from the static temperature and pressure measured inside the wheel-space on the stator at $r/b = 0.958$.

In both wheel-spaces purge air (sometimes seeded with CO_2) was introduced independently at a low radius ($r/b = 0.642$) through an inlet seal. By means of control

valves, a wide range of non-dimensional sealing flow rates, Φ_0 could be achieved. The annulus flow entering the turbine, along with the sealing flows entering each of the wheel-spaces, were measured and controlled using thermal mass-flow meters to an accuracy of ±1% of the full-scale range.

Parameters	**Disc Speed (RPM)**	
	3000	**4000**
Rotational Reynolds Number, $\mathbf{Re}_\phi$	7.2×10^5	1.0×10^6
Axial Reynolds Number, $\mathbf{Re}_w$	2.1×10^5	2.9×10^5
Flow Coefficient, C_F	0.293	
Vane exit Mach Number, M	0.24	0.32

Table 1: Test rig operating conditions

5.2 Experimental measurements

CO_2 was used throughout the test section as a tracer gas. As illustrated in Figure 5, the radial distribution of concentration was measured along the stator and, by means of hypodermic probes, in the core of both wheel-spaces at z/S = 0.25. Although not presented in this paper, at C_F = 0.293 the distribution of effectiveness in the wheel-space has been shown to be independent of Re_ϕ and circumferential position [2].

Concentration was also measured along a radial traverse of the mainstream annulus and into the rim seal region. The probe was a simple, stainless-steel hypodermic tube of 1.0 mm outer diameter. The traverse from the outer casing of the annulus to the seal clearance is illustrated as an inset in Figure 5. A larger hypodermic tube (1.7 mm outer diameter) was used to check that the probe and gas-extraction rate [14] did not influence the data collected.

In all cases the gas was extracted by a pump, which delivered samples to a Signal Group 9000MGA multi-gas analyser. The gas analyser had a repeatability and a linearity of better than ±1% and 0.5% of the full-scale range respectively.

5.3 Geometric features of radial-clearance seals

The split-ring and modular design of the test section allowed complex rim seal geometries to be tested expediently and efficiently; in this paper generic, radial-clearance seals with no commercial proprietary were used in both wheel-spaces. Figure 6 shows the geometric configuration of this seal with important dimensions listed in Table 2.

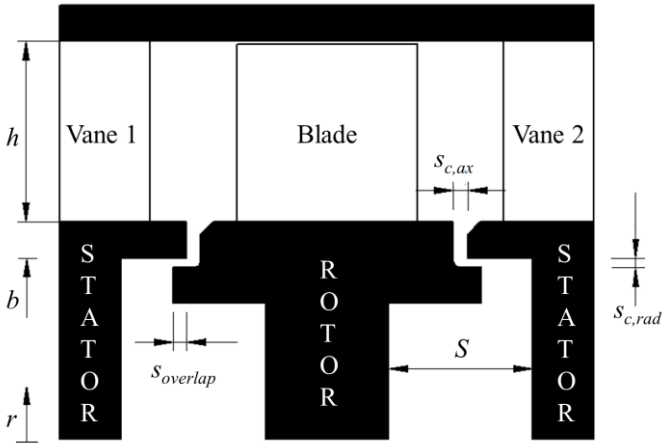

Figure 6: Radial-clearance seal configuration in the upstream and downstream wheel-spaces

Parameter	Dimension (mm)
h	25
b	190
S	20
$s_{c,ax}$	2
$s_{c,rad}$	1.28
$s_{overlap}$	1.86

Table 2: Dimensions of radial-clearance seal

6 RESULTS

In this section, the re-ingestion of upstream egress into the downstream wheel-space is reported using gas concentration measurements. To separate the *disturbance* and *carry-over* effects, two sets of experiments were conducted for a range of upstream and downstream sealing flow rates: *upstream-unseeded* and *upstream-seeded* tests. For the

latter experiments, the upstream sealing flow was seeded with 3% CO_2 ($c_{0,u}$ = 0.03); the upstream annulus flow was unseeded but with an inherent concentration ($c_{a,u}$ ~ 0.0004) measured at the entry to the turbine. All experiments were conducted with the radial-clearance seal in both wheel-spaces and at the two operating conditions shown in Table 1.

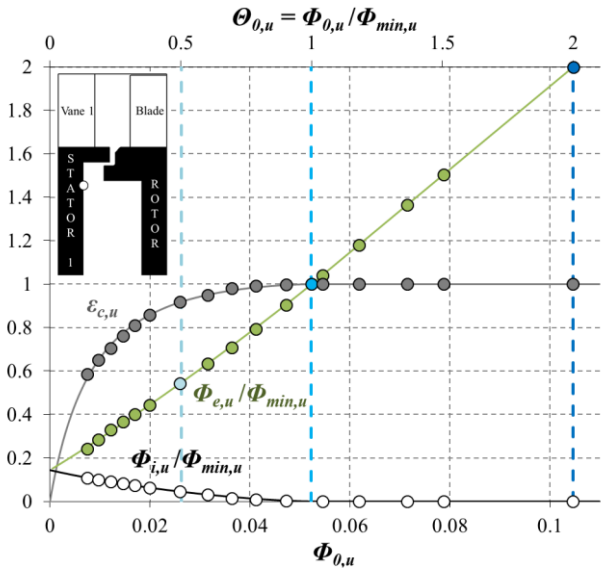

Figure 7: Distributions of concentration effectiveness, ingress and egress flow ratios with non-dimensional sealing flow rate in the upstream wheel-space (Symbols denote data; lines are theoretical orifice-model fits)

Figure 7 sets up the re-ingestion experiments by showing the variation of concentration effectiveness, the amount of ingress and most importantly the amount of egress with $\Phi_{0,u}$ in the upstream wheel-space. The concentration measurements were made on the upstream stator at r/b = 0.958, as indicated on the silhouette. As expected, $\varepsilon_{c,u}$ increases with increasing $\Phi_{0,u}$ as the sealing flow pressurises the wheel-space and reduces ingress through the rim seal. A theoretical effectiveness curve, Eq. (3.2), was fitted to this experimental data and there is good agreement with experiment. $\Theta_{0,u}$, the ratio of $\Phi_{0,u}/\Phi_{min,u}$ based on this theoretical fit is shown on a secondary axis.

Highlighted in the figure are three conditions used in the re-ingestion experiments, corresponding to $\Phi_{0,u}/\Phi_{min,u}$ = ½, 1 and 2. At $\Phi_{0,u}/\Phi_{min,u}$ = ½, ingress occurs and $\varepsilon_{c,u}$ ≈ 0.9. Ingress is prevented when $\Phi_{0,u} = \Phi_{min,u}$ and all the sealing flow leaves the wheel-space as egress. By definition $\varepsilon_{c,u}$ cannot reach a value greater than 1 therefore at $\Phi_{0,u}/\Phi_{min,u}$ = 2 the egress leaves the wheel-space with the same concentration as the $\Phi_{0,u} = \Phi_{min,u}$ case but with twice the flow rate.

6.1 Effectiveness measurements in the annulus

Figure 8 shows the radial variation of the effectiveness in the annulus, geometrically aligned with the silhouette of the turbine passage. The vertical axis is the non-dimensional radius which extends from $r/b = 1$ under the blade platform to $1.03 \leq r/b \leq 1.16$ across the annulus of height h = 25 mm. This data was collected using the hypodermic probe at two axial locations either side of the rotor blades with seeded sealing flow supplied to the upstream wheel-space with $\Phi_{0,u} = \Phi_{min,u}$, $c_{0,u}$ = 0.03 and $\varepsilon_{c,u}$ = 1.

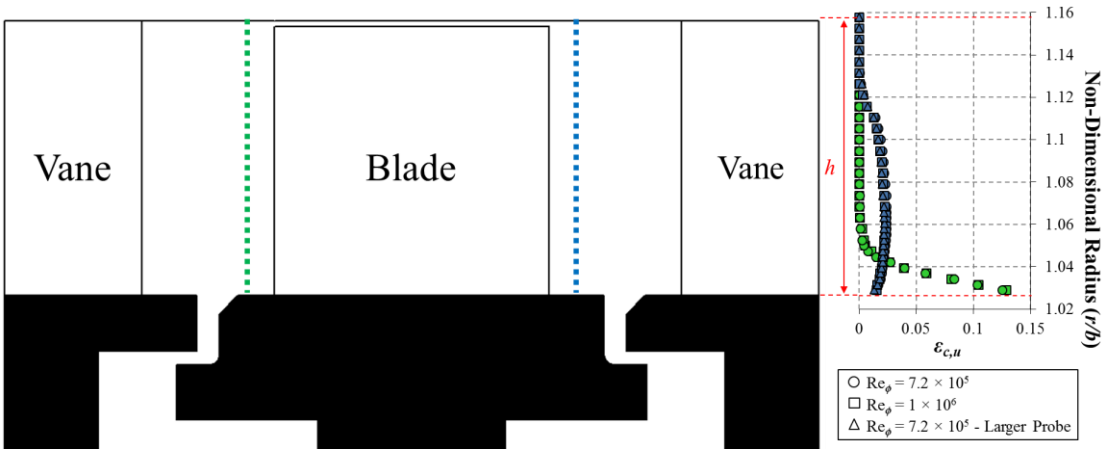

Figure 8: Measurements of upstream concentration effectiveness in the annulus either side of the rotor blades ($\Phi_{0,u} = \Phi_{min,u}$)

The effectiveness is based on the local concentration measured by the probe (c) relative to the concentration of the egress from the upstream wheel-space:

$$\varepsilon_{c,u} = \frac{c - c_{a,u}}{c_{0,u} - c_{a,u}} \tag{6.1}$$

In particular, $\varepsilon_{c,u} = 1$ when $c = c_{0,u}$ (indicating there has been no mixing of the egress and mainstream, and the local flow is entirely from the upstream wheel-space) and $\varepsilon_{c,u} = 0$ when $c = c_{a,u}$ (indicating the egress is not present in the annulus).

The data collected along the radial traverse upstream of the rotor blades (green dotted line) is shown in green, measured halfway between the downstream face of the rim seal and the blade leading-edge. At this relatively short distance downstream, a maximum $\varepsilon_{c,u} = 0.125$ was measured near the rotor platform. This reveals that there has been strong mixing between the egress and the mainstream annulus. The effectiveness reduces radially as the egress mixes further with the annulus flow, indicating a concentration boundary layer thickness of $0.18h$ ($1.03 \leq r/b \leq 1.05$). Data collected at the two operating points shows the concentration profile is invariant with Re_ϕ. The measurements also suggests there might be a film-cooling benefit on the rotor platform as well as aerodynamic mixing losses.

Scobie *et al.* [15] present measurements using the probe in the seal clearance which show $\varepsilon_{c,u} \sim 0.3$ and with the distribution of concentration dependent on the relative position of the upstream vane; this asymmetry is attenuated significantly but still persists at the upstream measurement location (green dotted line) shown in Figure 7.

The concentration measurements downstream of the rotor blades are shown in blue. The radial traverse (blue dotted line) was at an axial position halfway between the blade trailing-edge and the upstream face of the rim seal clearance. The sealing flow is observed to migrate radially to $0.8h$ ($r/b = 1.13$) as it is entrained into the blade passage vortex (see Figure 2). Mixing with the mainstream annulus has reduced the maximum

effectiveness to $\varepsilon_{c,u}$ = 0.024; close to the rotor platform this has diminished to 0.015 but suggests that some degree of film cooling might still be effective downstream of the rotor.

As in the case upstream, data collected at the two operating points shows the concentration profile is invariant with Re_ϕ. The data collected with the two different-sized probes (outer diameters 1.0 and 1.7 mm) collapse to a single curve, which confirms that the probe did not affect the concentration measurements.

6.2 Effectiveness measurements through the rim seal

Figure 9 shows the radial variation of concentration effectiveness ($\varepsilon_{c,u}$) across the annulus and within the wheel-space downstream of the rotor. The data was collected under the same conditions as those presented in Figure 7, *i.e.* seeded upstream egress with $\Phi_{0,u} = \Phi_{min,u}$. Note, however the change in scale of the axis, and the measurement plane is further downstream. The measurements were taken from the taps on the downstream stator surface (squares), from hypodermic probes in the rotating-core (diamonds) at z/S = 0.25, and from the probe traverse across the annulus and through the centre of the rim seal clearance (circles). The data is geometrically aligned with the silhouette of the rig cross-section; it should be noted the external flow is from left to right (*i.e.*, from the rotor to the stator) and the probe traverse is shown as the vertical dotted line.

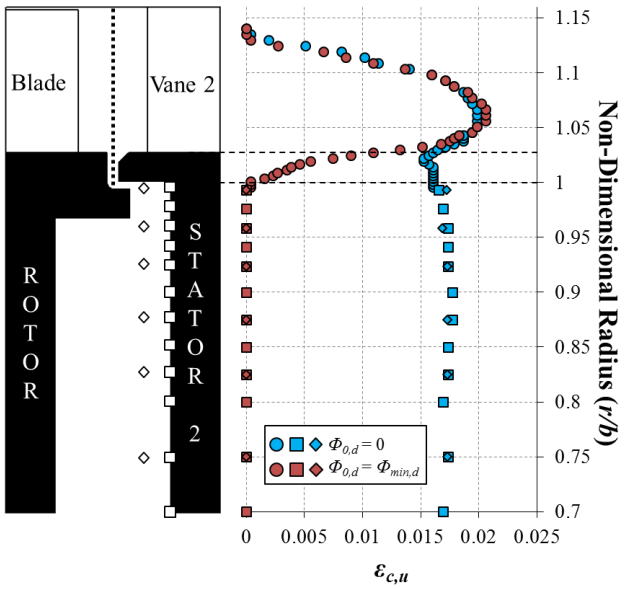

Figure 9: Effect of downstream sealing flow rate on radial distribution of re-ingestion in the downstream annulus and wheel-space for $\Phi_{0,u} = \Phi_{min,u}$ (squares: stator-wall; diamonds: rotating-core; circles: probe measurements)

The experiments were conducted with unseeded downstream sealing flow ($c_{0,d} = 0$) for two extremes: zero downstream sealing flow (blue), corresponding to the case of maximum ingress and re-ingestion; and the fully-sealed case (red) where $\Phi_{0,d} = \Phi_{min,d}$ corresponding to zero ingress, hence no re-ingestion. The results for the former case clearly demonstrate significant re-ingestion, which decreases with increasing $\Phi_{0,d}$ as the wheel-space is pressurised and reduces the ingress of seeded flow from the annulus.

The probe measurements demonstrate that mixing between the seeded re-ingestion and unseeded downstream egress takes place in the rim seal region. With no downstream sealing flow, re-ingestion penetrates the wheel-space. The concentration in the rotating core and the stator wall are equal and indicate 1.8% of the seeded upstream sealing flow is re-ingested downstream; the effectiveness is invariant with radius and these measurements are consistent with the expected flow structure illustrated in Figure 2.

The measurements for the sealed wheel-space exhibit a similar trend but with more intense mixing in the rim seal clearance. In the annulus the concentration is virtually the same for the two cases, indicating a weak interaction between the egress and mainstream.

The annulus-concentration profile shown in Figure 9 was collected using upstream-seeded egress with $\Phi_{0,u}/\Phi_{min,u} = 1$. This profile is reproduced in Figure 10, along with data conducted with upstream seeding at $\Phi_{0,u}/\Phi_{min,u} = ½$ and 2. The radial migration of the egress is observed to increase with increased egress momentum. The reduction in annulus concentration for $\Phi_{0,u}/\Phi_{min,u} = ½$ is consistent with the fact that the egress concentration ($c_{e,u}$) decreases as $\Phi_{0,u}$ decreases. However, when $\Phi_{0,u} > \Phi_{min,u}$ then the egress concentration will be unchanged so that $c_{e,u} = c_{0,u}$. Under these circumstances, any fluid entrained into the downstream ingress from the boundary layer on the blade platform will have a concentration which is invariant with $\Phi_{0,u}$.

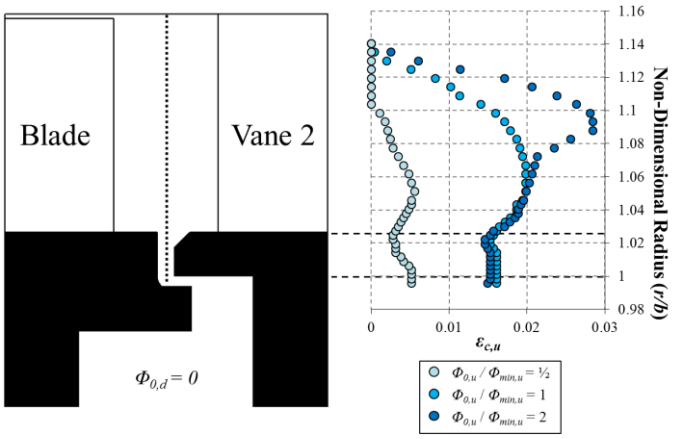

Figure 10: Effect of upstream sealing flow rate on radial distribution of re-ingestion in the downstream annulus and rim seal region for $\Phi_{0,d} = 0$

6.3 Re-ingestion: Disturbance effect

This section describes upstream-unseeded tests but with the downstream sealing flow seeded with tracer gas. The definitions of $\varepsilon^*_{c,d}$ and $\varepsilon_{c,d}$ are given by Eqs. (4.3) and (4.4) respectively.

Figure 11 shows the variation of effectiveness with $\Phi_{0,d}$ in the downstream wheel-space for the datum case without upstream sealing flow, i.e. $\Phi_{0,u}/\Phi_{min,u} = 0$. The concentration measurements were made on the downstream stator at $r/b = 0.958$, as indicated on the silhouette. Note from the discussion of the flow structure this measurement represents the concentration at all radii on the stator and in the core. As expected, $\varepsilon_{c,d}$ increases with increasing $\Phi_{0,d}$ as the sealing flow pressurises the wheel-space and reduces ingress through the rim seal. A theoretical effectiveness curve, Eq. (3.2), was fitted to this experimental data and once again there is good agreement with experiment.

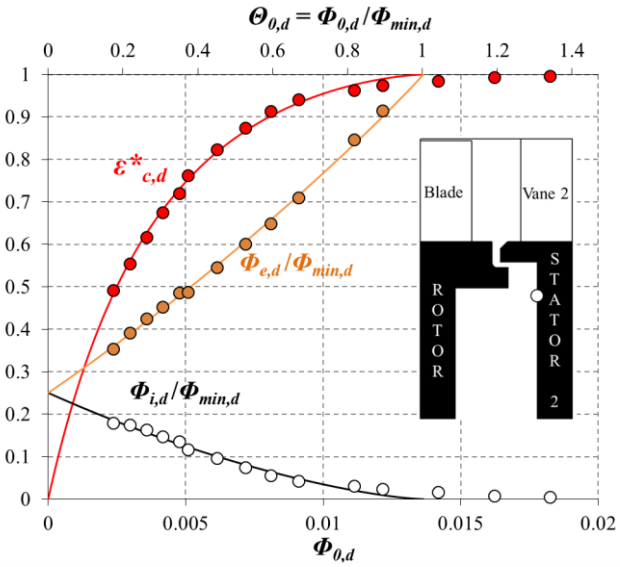

Figure 11: Distributions of downstream concentration effectiveness, ingress and egress flow ratios for the datum case without upstream sealing flow (Symbols denote data; lines are theoretical orifice-model fits)

Also presented in Figure 11 are the non-dimensional ingress and egress ratios, determined using Eqs. (3.3) and (3.4) respectively. These give an indication of the maximum ingested flow as a proportion of the minimum sealing flow rate required to prevent ingestion. With no sealing flow ($\Phi_{0,d} = 0$) all ingress entering the wheel-space must leave as egress and therefore $\Phi_{i,d} = \Phi_{e,d}$. At $\Phi_{0,d} = \Phi_{min,d}$, ingestion is prevented and all sealing flow leaves the wheel-space as egress.

Figure 12 shows the same variation of effectiveness in the downstream wheel-space for three *upstream-unseeded* flow conditions: $\Phi_{0,u}/\Phi_{min,u}$ = ½, 1 and 2. The measured effectiveness is shown to be invariant with the unseeded upstream sealing flow rate and the data collapse onto a single curve. This shows the *disturbance effect* is not significant over a wide range of upstream egress flow.

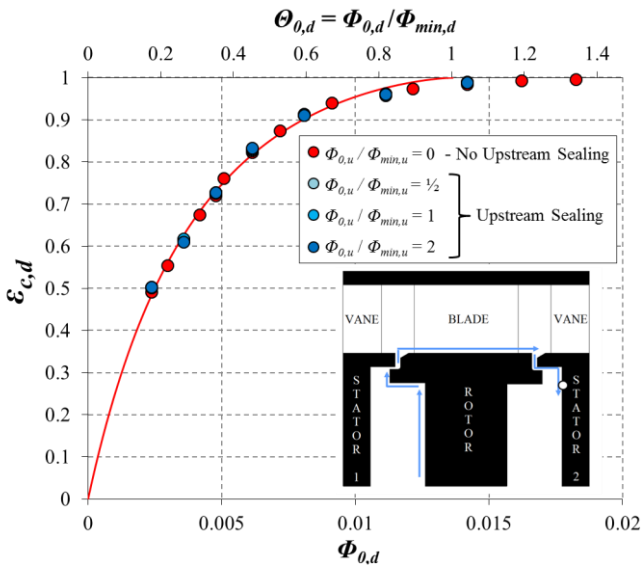

Figure 12: Downstream measurements of concentration effectiveness with sealing flow rate for four values of unseeded upstream sealing flow (Symbols denote data; line is theoretical orifice-model fit)

6.4 Re-ingestion: carry-over effect

This section describes *upstream-seeded* tests with the downstream sealing flow also seeded with the same tracer gas. Figure 13 illustrates the effect of the upstream egress which is re-ingested into the downstream wheel-space. For $\Phi_{0,u}/\Phi_{min,u}$ = ½, 1 and 2, an increase in effectiveness is measured relative to the datum case $\Phi_{0,u}$ = 0. The datum case is equivalent to the unseeded upstream tests described in Section 6.3.

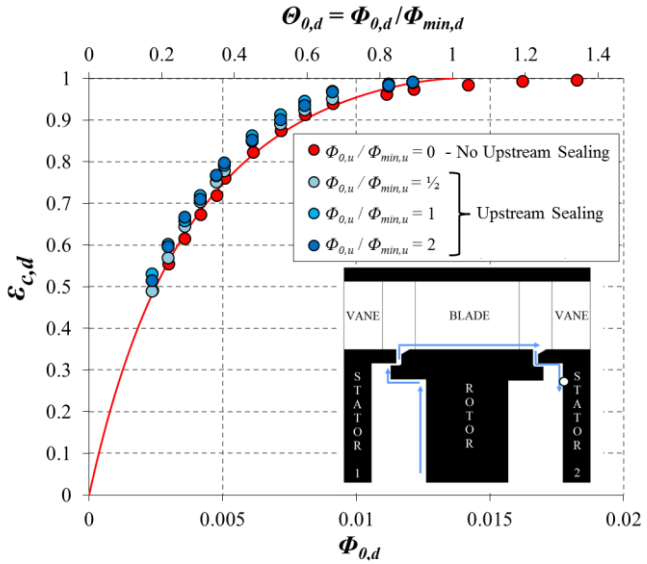

Figure 13: Downstream measurements of concentration effectiveness with sealing flow rate for four values of seeded upstream sealing flow (Symbols denote data; line is theoretical orifice model fit)

Figures 14 and 15 show the measured variation of χ with $\Phi_{0,d}$ and $\varepsilon_{c,d}$ respectively. Eq. (4.15) reveals that χ has a physical significance as the carry-over fraction, *i.e.* the ratio of mass flow rate of upstream egress (with upstream concentration $c_{e,u}$) entrained into the downstream ingress. When $\Phi_{0,d}$ = 0 (and $\varepsilon_{c,d} \rightarrow 0$), the ingress is at a maximum and χ is at a minimum. As $\Phi_{0,d} \rightarrow \Phi_{min,d}$ (and $\varepsilon_{c,d} \rightarrow 1$) then the ingress will contain an increasing fraction of upstream egress so that $\chi \rightarrow 1$. This behaviour can be seen in Figures 14 and 15.

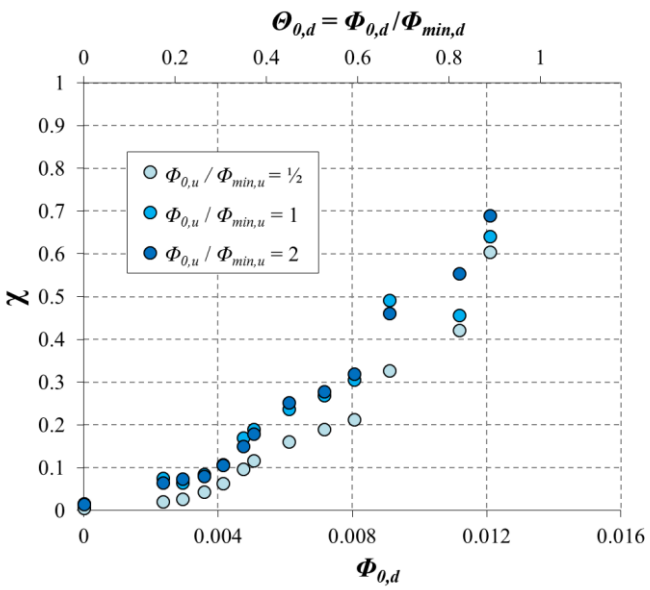

Figure 14: Measured variation of χ with downstream sealing flow rate for three values of seeded upstream sealing flow rate

It can also be seen that, relative to $\Phi_{0,u}/\Phi_{min,u} = 1$, χ decreases when $\Phi_{0,u}/\Phi_{min,u} = ½$; this is consistent with the fact that $c_{e,u}$ decreases as $\Phi_{0,u}$ decreases and ingestion takes place upstream (as shown in Figure 7). However, when $\Phi_{0,u} > \Phi_{min,u}$ then the egress concentration will be unchanged so that $c_{e,u} = c_{0,u,}$. The fact that doubling $\Phi_{0,u}$ from $\Phi_{min,u}$ to $2\times\Phi_{min,u}$ has no significant effect on χ is surprising as it seems reasonable to expect that the mass flow of egress entrained into the downstream ingress would increase as $\Phi_{e,u}$ increases. One possible explanation is that the carry-over fluid emanates from the boundary layer on the blade platform where the concentration is invariant if $\Phi_{e,u} > \Phi_{min,u}$, and there is evidence in Figure 10 that this is the case.

Engine designers typically operate at a sealing effectiveness ~ 0.95. Figure 15 suggests that under these circumstances χ ~ 0.3. The mass-transfer analogy therefore suggests that the enthalpy transfer from the relatively cold fluid from the upstream egress that is entrained into the downstream ingress would significantly reduce the adverse effect of the ingress.

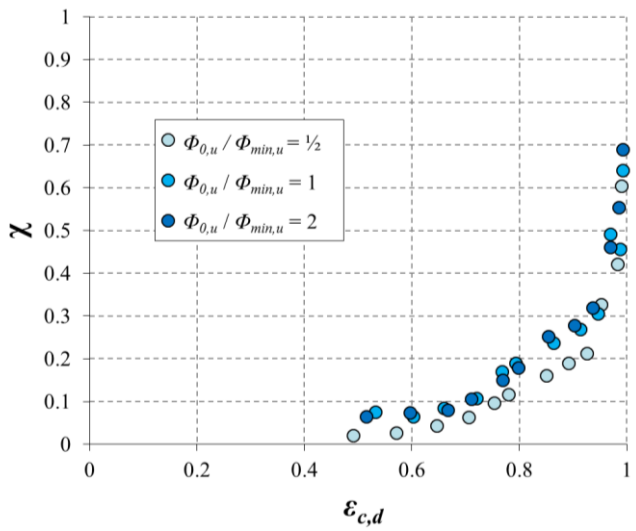

Figure 15: Measured variation of χ with non-dimensional downstream concentration effectiveness for three values of upstream sealing flow rate

6.5 Significance, limitations and impact

The paper has examined ingress through a downstream rim seal of flow which is mixed with upstream egress. Here a theoretical mixing model has been developed from first principles and validated by experimental measurements. The experiments have been presented in terms of non-dimensional variables (ε_c, C_F, Φ_o, Re_ϕ and χ) which provide meaningful data to the engine designer by scaling through theoretical models [*e.g.*, 5]. A concentration probe has successfully collected data in the annulus, wheel-space within the seal clearance. The research shows that the upstream purge does not significantly disturb the fluid dynamics but only partially mixes with the annulus flow near the downstream seal, with the ingested fluid emanating from the boundary layer on the blade platform. For the first time, a method to quantify the mass fraction of the fluid carried over from upstream egress into downstream ingress (χ) has been presented and measured. The degree of any disturbance or χ will likely depend on the turbine geometry (vanes, blades, end-wall contouring and seals) and throat Mach number. The model and measurements used here cannot account for heat transfer, which will

attenuate the favourable effect of re-ingestion. Current engine design practice uses unsteady-computational predictions which are unreliable if not carefully validated, and accurate calculations of heat transfer probably do not exist. The data and model presented in this paper provide insight and a means of accurate validation for any computational code operating under adiabatic conditions; successful validation would provide confidence to progress to calculations with heat transfer. This paper is significant to engine design practice as the re-ingestion will have an impact on purge-flow requirements and performance.

7 CONCLUSIONS

Re-ingestion in a 1.5-stage gas turbine rig, with radial-clearance seals, was studied using gas concentration measurements; CO_2 seeding was injected into the upstream and downstream sealing flows. Concentration measurements on the stationary surfaces of both wheel-spaces were complemented by radial traverses using a probe in the annulus and within the seal clearance.

- For the first time, a method to quantify the mass fraction of the fluid carried over from upstream egress into downstream ingress (χ) has been presented and measured.
- By comparing the sealing effectiveness for the downstream wheel-space with and without CO_2 seeding in the upstream sealing flow, values of χ were calculated over a range of flow rates.
- It was shown that the upstream purge does not significantly disturb the fluid dynamics but only partially mixes with the annulus flow near the downstream

seal, with the ingested fluid emanating from the boundary layer on the blade platform.

- It was shown that χ increased as the downstream sealing flow rate increased, and values of $\chi \sim 0.3$ would be typical in the engine.
- From the analogy between heat and mass transfer, it was concluded that the fluid carry-over from the upstream egress into the downstream ingress could significantly reduce the adverse effect of ingress in the downstream wheel-space. Note that heat transfer effects were not assessed quantitatively.

ACKNOWLEDGMENT

The research described here was supported by the Engineering and Physical Sciences Research Council (EPSRC) and Siemens AG. Data Access: Due to confidentiality agreements with research collaborators, supporting data can only be made available to bona fide researchers subject to a nondisclosure agreement. Details of how to request access are available at the University of Bath data archive: http://dx.doi.org/10.15125/BATH-00116.

NOMENCLATURE

a	speed of sound *(m/s)*
b	radius of seal (*m*)
c	concentration of tracer gas (*%*)
$\tilde{c}$	mixed-out concentration
$C_{d,e}$	discharge coefficient for egress
$C_{d,i}$	discharge coefficient for ingress
C_F	flow coefficient ($W/\Omega b$)

$C_{w,0}$ nondimensional sealing flow rate (= $\dot{m}/\mu b$)

G_c seal-clearance ratio (= $s_{c,ax}/b$)

h height of annulus *(m)* and enthalpy *(J/kg)*

$\dot{m}$ mass flow rate (*kg/s*)

M Mach number

r radius (*m*)

Re_w axial Reynolds number in annulus based on radius (= $\rho W b/\mu$)

Re_ϕ rotational Reynolds number (= $\rho \Omega b^2/\mu$)

s_c seal clearance (*m*)

S axial clearance between rotor and stator (*m*)

U bulk mean radial seal velocity (= $\dot{m}_0/2\pi\rho b s_c$)

W axial velocity in annulus (*m/s*)

z axial coordinate (*m*)

Γ_c ratio of discharge coefficients (= $C_{d,i}/C_{d,e}$)

ε effectiveness

ε_c concentration effectiveness

Θ_0 sealing flow ratio (= Φ_0/Φ_{min})

Θ_e egress flow ratio (= Φ_e/Φ_{min})

Θ_i ingress flow ratio (= Φ_i/Φ_{min})

μ dynamic viscosity (*kg/ms*)

ρ density (kg/m^3)

Φ_0 non-dimensional sealing parameter (= $U/\Omega b$)

Φ_{min} minimum value of Φ_0 to seal wheel-space

Φ_{min}' value of Φ_0 when ε_c = 0.95

χ re-ingestion mass fraction

Ω	angular speed of rotating disc (*rad/s*)

Subscripts

a	annulus
ax	axial
c	concentration
d	downstream
e	egress
i	ingress
min	minimum
rad	radial
s	stator surface
u	upstream
0	sealing flow

Superscripts

*	value for upstream-unseeded case
'	value re-ingested

References

[1] Carey, C., Inderwildi, O. and King, D., 2009, "Sealing Technologies – Signed, Sealed and Delivering Emissions Savings," Aviation and the Environment, 4, pp. 44-48.

[2] Patinios, M., Scobie, J. A., Sangan, C. M., Owen, J. M. and Lock, G. D., 2017, "Measurements and Modelling of Ingress in a New 1.5-Stage Turbine Research Facility," ASME J. Gas Turb. Pwr., 139, p.012603.

[3] Langston, L. S., 2001, "Secondary flows in axial turbines - a review," Annals of the New York Academy of Sciences, 934(1), 11-26.

[4] Scobie, J. A., Sangan, C. M., Owen, J. M., and Lock, G. D., 2016, "Review of Ingress in Gas Turbines," ASME J. Gas Turb. Pwr., 138(12), p.120801.

[5] Owen, J. M., 2011, "Prediction of Ingestion through Turbine Rim Seals. Part II: Externally Induced and Combined Ingress," ASME J. Turbomach., 133(3), 031006.

[6] Sangan, C. M., Pountney, O. J., Zhou, K., Wilson, M., Owen, J. M., and Lock, G. D., 2013, "Experimental Measurements of Ingestion through Turbine Rim Seals. Part 1: Externally-Induced Ingress," ASME J. Turbomach., 135(2), 021012.

[7] Wisler, D. C., 1985, "Aerodynamic effects of tip clearance, shrouds, leakage flow, casing treatment and trenching in compressor design blading design in the endwall region'. Von Karman Institute for Fluid Dynamics Lecture Series 1985-05.

[8] Bayley, F. J, Childs, P. R. N, 1994. 'Air temperature rises in compressor and turbine stator wells.' ASME Paper 94-GT- 185.

[9] Ozturk, H.K., Childs, P. R. N., Turner, A. B., Hannis, J. M. and Turner, J. R., 1998, A three dimensional computational study of windage heating within an axial compressor stator well," ASME Paper No. 98-GT-119.

[10] Specific Targeted Research Project, 2006, "Annex I—'Description of Work'," Main Annulus Gas Path Interactions (MAGPI), Proposal/Contract No. 30874.

[11] Georgakis, C., Whitney, C., Woolatt, G., Stefanis, V., and Childs, P., 2007, "Turbine Stator Well Studies: Effect of Upstream Egress Ingestion," ASME Paper No. GT2007-27406.

[12] Eastwood, D., Coren, D. D., Long, C. A., Atkins N. R., Childs, P. R. N., Scanlon, T. J. and Guijarro-Valencia, A., 2012, "Experimental Investigation of Turbine Stator Well Rim Seal, Re-Ingestion and Interstage Seal Flows Using Gas Concentration Techniques and Displacement Measurements," ASME J. Turbomach., 134(8), 082501.

[13] Guijarro-Valencia, A., Dixon, J. A., Da Soghe, R., Facchini, B., Smith, P. E. J., Munoz, J., Eastwood, D., Long, C. A., Coren, D. D. and Atkins N. R., 2012, "An Investigation into Numerical Analysis Alternatives for Predicting Re-ingestion in Turbine Disc Rim Cavities," ASME Paper GT2012-68592.

[14] Clark, K., Barringer, M. and Thole, K., 2016, "Using a tracer gas to quantify sealing effectiveness for engine realistic rim seals," ASME Paper GT2016-58095.

[15] Daniels, W. A., Johnson, B. V., Graber, D. J. and Martin, R. J., 1992, "Rim Seal Experiments and Analysis for Turbine Applications," ASME J. Turbomach., 114(2), pp. 426-432.

[16] Scobie, J. A., Hualca, F. P., Sangan, C. M. and Lock, G. D., 2017, "Egress interaction through turbine rim seals," ASME Paper GT2017-64632.